Monte Carlo N-Particle Method Dose Calculations Using Gold Nanoparticles in Cobalt-60 Radiation Therapy

J.T.P. Cruz[1], A.L. Rodriguez[2], J.D. Trono[3*]
[1]St Luke's College of Medicine - WHQM, Cathedral Heights, Sta. Ignaciana St., Quezon City , Philippines;
[2]De La Salle Health Sciences Institute, Congressional Ave., Pasong Lawin, Dasmarinas, Cavite, Philippines; and
[3]Physics Department, De La Salle University, 2401 Taft Avenue, Manila, Philippines
*Email: jade.trono@dlsu.edu.ph

In this paper, amplification in dose due to the presence of gold nanoparticles was quantified using Monte Carlo N-Particle (MCNP) simulation. Simulation models included the irradiation of a 30 cm × 30 cm × 15 cm pure-water—volume phantom with a beam of 1.17 MeV and 1.33 MeV Cobalt spectral emissions as source. Planar and concentric water panel detectors placed at a distance of intervals of 0.1 cm from the center and the surface were used to obtain radial and depth doses within. To verify the accuracy of the program codes and the phantom specifications used, baseline data using water phantom were compared to calibration data. Amplification in irradiation of a water phantom with spherical tumor and irradiation of a water phantom with varying concentrations GNP-embedded tumor was also determined. Statistical comparisons were done using analysis of variance (ANOVA) and T-test to determine the relationships among the data parameters garnered. As expected, GNPs amplified radiation dose through photoelectric effect showing an increase of 0.407% for 1 mg/g and 8.54% for 7 mg/g GNP concentrations. 1 mg/g and 7 mg/g GNP concentrations recorded 68.68% and 104.81% difference, respectively, in comparison with planar doses achieved in model B. A percent of difference of 128.51%, on the other hand, was obtained when planar doses of 1 mg/g and 7 mg/g GNP-concentrations were compared.

1. INTRODUCTION

Cancer remains to be a worldwide killer (Anand et al., 2008). According to the recent statistics released by the Philippine Cancer Society (PCS), at least 200,000 Filipinos suffer from cancer every year (Laudico, Esteban, Redaniel, Mapua, & Reyes, 2005) and by 2020, the world population is expected to have increased by 7.5 billion, and of this number, approximately 15 million new cancer cases will be diagnosed and 12 million cancer patients will die (Bray & Moller, 2006). Hence, studies focusing on new ways of diagnosing and treating cancer with the integration of nanotechnology offer an extraordinary and paradigm-changing opportunity in making significant advances (Cuenca et al., 2006) towards better cancer prognosis.

These recent biomedical interests in nanoparticles spurred due to their profound influence on cell - nanoparticle interactions (Raha, Paunesku, & Woloschak, 2011) such as depolarization of cell membranes and modulation of calcium release in cells in vitro caused by electropositive nanoparticles and

selection of positively charged nanoparticles over the other nanoparticles as prey to neutrophil extracellular traps in vivo (Arvizo et al., 2010; Cuenca et al., 2006).

To realize the capability of nanoparticles in affecting more than one organ or tissue (pluripotentiality), attachment of multiple molecules on every nanoparticle is desired. Researches about the use of cell-penetrating peptides to deliver nanomaterials, specifically gold nanoparticles, have been done and successfully returned positive outcomes in enhancing the doses in tumor (Cuenca et al., 2006).

1.1. Gold Nanoparticles (GNPs)

GNPs, which are biologically nonreactive, nontoxic, and molecularly stable (Bartneck, Keul, Zwadlo-Klarwasser, & Groll, 2010; McMahon et al., 2011), have been widely used as biomarkers or image and dose enhancers (Trono et al., 2011). It has high mass attenuation coefficient as well, which enabled it to have a high chance of photon encounter due to its compact molecules (Cho, Jones, & Krishnan, 2009). GNPs were found not to induce any universally cell-specific response even in the absence of any specific functionalization (Bartneck et al., 2010) and are eliminated significantly within the body in 24 hours (Raha et al., 2011). Due to its high Z-value and great surface-volume ratio, photoelectric effect is much favorable to occur (McMahon et al., 2011) and hence attributes a significant increase in photoelectron fluence during x-ray irradiation (Cho et al., 2009). Thus, these could be best utilized in radiation imaging and therapy (Chantler, 2005).

Typically, GNPs are introduced at the center of the volume to maximize their biological effectiveness on surrounding cells through bystander effect at the microscopic level (Bartneck et al., 2010; Rahman et al., 2009). In a study by Rahman et al. (2009), radiation effects are found to be enhanced by the presence of GNPs and have no significant toxicity as dictated by animal experiment (Hainfeld, Dilmanian, Slatkin, & Smilowitz, 2008). These findings provided positive support for the use of GNPs in radiation therapy. However, amplification in radiation caused by the introduction of GNPs in tumors was never quantified in any of the researches mentioned. This study aims to quantify the effect of GNPs on dose amplification for varying concentrations of GNPs in tumor volumes.

1.2. Monte Carlo N-Particle (MCNP)

In order to be able to maximize the use of GNPs as one of the dose enhancement tools in imaging and therapy, at least, an approximate of the amplification rate per concentration is needed. However limited resources, a high probability of uncertainties, and costly and time-consuming experiments cause the determination of amplification rate to be impractical. This study presents a solution through an alternative way aimed to minimize the expense and to acquire more accurate results through computer simulations by using the MCNP computational method.

MCNP is capable of predicting outcomes of problems that involve radiation of specific particles such as neutron, photon, electron, or coupled neutron/photon/electron transport (X-5MonteCarloTeam, 2003a, 2003b, 2003). Through the use of MCNP, one can simulate particle transport and eventually approximate the dose received by the target, and everything within the specified range identifying the amplification rate brought by the varying concentrations of GNPs can be known (Yusa, Jiang, Mizuno, & Uesaka, 2009).

2. METHODOLOGY

The amplification brought by the GNPs embedded on tumor volumes was quantified. Different models determined the trend of the absorbed radial and planar doses achieved by the selected target during cobalt-60 irradiation. All simulations used the MCNP Visual Editor in running MCNP5-defined codes, which were

composed of the title, surface, cell and data cards (Carter, et al, 2005).

Generally, all simulations (a) were composed of 30 cm × 30 cm × 15 cm water-volume phantom made of polymethyl methacrylate (PMMA, $C_5O_2H_8$), a material compatible with human tissue filled with four-component tissue of ICRU44 ("X-Ray Mass Attenuation Coefficients,"); (b) were irradiated by Cobalt-60 spectral emissions particularly, 1.17 MeV and 1.33 MeV; (c) collected radial doses along the transverse axis of the source (or phantom) between 1 and 10 cm by concentric annuli (0.1 cm high and 0.1 cm wide in the cross-sectional dimensions) with the energy deposition tally and were tracked until the radius of 100 cm (Figure 1); (d) measured incident doses from the center point tracking at (15.25, 75, 15.25); (e) run until 1×10^8 particles were tracked; (f) were set to an importance of physics simplification of photon interaction – allowing energy cut-offs and physics treatment necessary for photons; (g) were set to an energy of 0.0 MeV before simple physics was used and where no fluorescence was produced from the photoelectric interactions; and lastly, (h) included bremsstrahlung and Doppler broadening while coherent scattering was ignored.

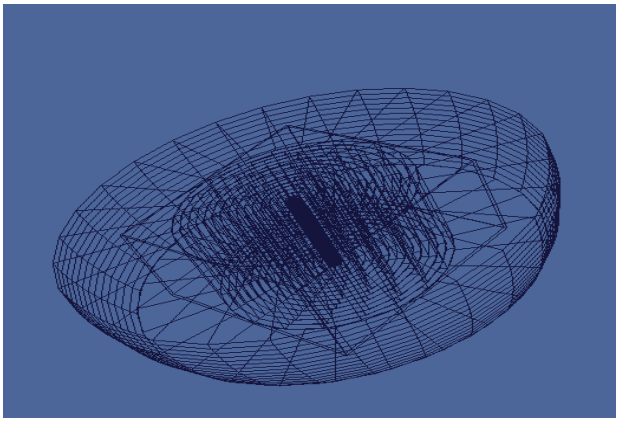

***Figure 1*: Ray-outline of the simulated phantom in the study.**

2.1. Model A: Irradiation of Phantom

Model A simply aims to simulate the published results on calibration of water phantom for cobalt-60 irradiation and to verify the MCNP5 codes by comparing the values achieved in the simulation with those of the published results (Juste, Miro, Gallardo, Verdu, & Santos, 2005). With this, coding for models B and C was made easier since only the cell materials needed modification. In MCNP simulation, a 10 cm × 10 cm field size beam of Co-60 was used (Figure 1).

2.2. Model B: Irradiation of Phantom With Spherical Tumor

Model B was synonymous to Model A except that a 1.8 cm-diameter spherical tumor at the center of the phantom was present. It must be noted that (a) the tumor in Model B does not have GNPs in it; (b) values obtained will not be compared to any experimental data and; (c) only a 5 cm × 5 cm beam field size was used. Model B served as the control setup of the study. Radial and depth doses received during Co-60 irradiation were simulated.

2.3. Model C: Irradiation of Phantom With Gold-Embedded Spherical Tumor

Model C is similar to Model B except that the central spherical tumor was embedded with GNPs of varying concentrations, specifically, 1 mg/g and 7 mg/g tumors. In this simulation, the GNPs were assumed to be equally distributed within the tumor. Also, it must be noted that (a) values obtained will not be compared to any experimental data (b) only a 5 cm × 5 cm beam field size was used. Radial and depth doses received during Cobalt-60 irradiation were measured. Obtained values in Models B and C were compared, analyzed and the amplification rate brought by varying GNP concentration was determined (Figure 1).

3. RESULTS AND DISCUSSION

The results obtained in MCNP simulation for Model A shows no significant difference as to the results obtained by Juste et al. (2005). Through ANOVA, a 95% confidence interval was achieved from the radiation dose values. These results assure the accuracy and precision of the code to be used as the base program for Models B and C.

The comparison of Models B and C, on the other hand, provided a positive amplification value with regards to the dose received by the tumor embedded with GNPs. Planar doses of 1 mg/g and 7 mg/g GNP concentrations recorded percentage differences of 68.68% and 104.81% respectively, when compared with the planar doses achieved in Model B while a percent difference of 128.51% was obtained when planar doses of 1 mg/g and 7 mg/g GNP concentrations were compared (Figure 3).

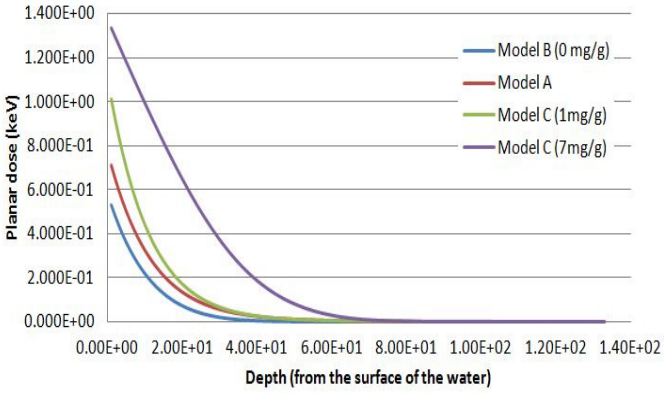

***Figure 3*: Comparison of the planar dose for Models A, B and C**

Figure 2 shows an amplification of the relative dose from the inner to outer cylindrical detector for different models. With Model B as the baseline, a steady increase in the planar dose was observed. Increase was observed optimal at 7 mg/g GNP concentration. Relative dose achieved by 1 mg/g and 7 mg/g GNP concentration compared with Model B garnered percent differences of 76.9% and 157% while the percent difference between 1 mg/g and 7 mg/g of GNP-concentration is 152%.

An increase in the dose received by the surrounding tissues has also been observed. This comparison proved that GNPs in tumor volumes would amplify the radiation doses in direct proportion to the gold concentration. GNPs amplified radiation dose through photoelectric effect showing an increase of 0.407% for 1 mg/g and 8.54% for 7 mg/g GNP concentrations.

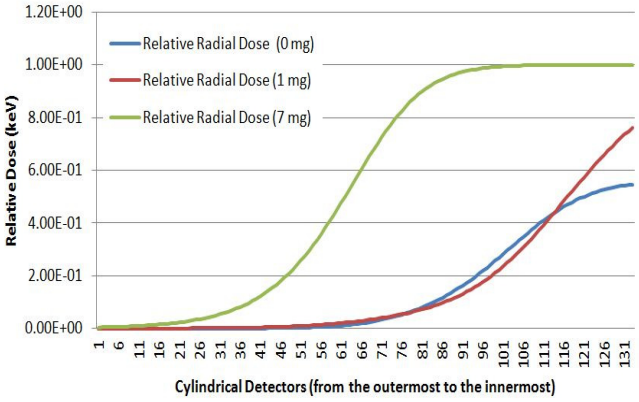

***Figure 2*. Comparison of the relative dose in keV for different GNP concentrations**

4. CONCLUSION

Theoretically, the localized amplification of dose within the tumor would be by virtue of the release of long-range photoelectrons and a shower of short-range Auger electrons of GNPs after the photon interaction (Anand et al., 2008). The presence of GNPs inside the tumor volume would make tumors radio-sensitive (Anand et al., 2008; Bray & Moller, 2006) making dose amplification more significant for its biological effectiveness. This study suggests the effectiveness of GNPs for dose amplification and provides the necessary data for the quantitative determination.

REFERENCES

Anand, P., Kunnumakara, A., Sundaram, C., Harikumar, K., Tharakan, S., Lai, O., . . . Aggarwal, B. (2008). Cancer is a

Preventable Disease that Requires Major Lifestyle Changes. *Pharmaceutical Research, 25*(9), 2097-2116. doi: 10.1007/s11095-008-9661-9

Arvizo, R. R., Miranda, O. R., Thompson, M. A., Pabelick, C. M., Bhattacharya, R., Robertson, J. D., . . . Mukherjee, P. (2010). Effect of nanoparticle surface charge at the plasma membrane and beyond. *Nano Lett, 10*(7), 2543-2548. doi: 10.1021/nl101140t

Bartneck, M., Keul, H. A., Zwadlo-Klarwasser, G., & Groll, J. (2010). Phagocytosis independent extracellular nanoparticle clearance by human immune cells. *Nano Lett, 10*(1), 59-63. doi: 10.1021/nl902830x

Bray, F., & Moller, B. (2006). Predicting the future burden of cancer. *Nat Rev Cancer, 6*(1), 63-74. doi: 10.1038/nrc1781

Chantler, C. T., Olsen, K., Dragoset, R.A., Chang, J., Kishore, A.R., Kotochigova, S.A., and Zucker, D.S. (2005). X-Ray Form Factor, Attenuation and Scattering Tables (version 2.1). Available: http://physics.nist.gov/ffast [Friday, 01-Feb-2013 05:58:31 EST]

Cho, S. H., Jones, B. L., & Krishnan, S. (2009). The dosimetric feasibility of gold nanoparticle-aided radiation therapy (GNRT) via brachytherapy using low-energy gamma-/x-ray sources. *Phys Med Biol, 54*(16), 4889-4905. doi: 10.1088/0031-9155/54/16/004

Cuenca, A. G., Jiang, H., Hochwald, S. N., Delano, M., Cance, W. G., & Grobmyer, S. R. (2006). Emerging implications of nanotechnology on cancer diagnostics and therapeutics. *Cancer, 107*(3), 459-466. doi: 10.1002/cncr.22035

Hainfeld, J. F., Dilmanian, F. A., Slatkin, D. N., & Smilowitz, H. M. (2008). Radiotherapy enhancement with gold nanoparticles. *J Pharm Pharmacol, 60*(8), 977-985. doi: 10.1211/jpp.60.8.0005

Juste, B., Miro, R., Gallardo, S., Verdu, G., & Santos, A. (2005). Considerations of MCNP Monte Carlo code to be used as a radiotherapy treatment planning tool. *Conf Proc IEEE Eng Med Biol Soc, 3*, 2828-2831. doi: 10.1109/iembs.2005.1617062

Laudico, A., Esteban, D., Redaniel, M., Mapua, C., & Reyes, L. (2005). *Philippine Cancer Facts and Estimates*. Manila: Philippine Cancer Society.

McMahon, S. J., Hyland, W. B., Muir, M. F., Coulter, J. A., Jain, S., Butterworth, K. T., . . . Currell, F. J. (2011). Biological consequences of nanoscale energy deposition near irradiated heavy atom nanoparticles. *Sci Rep, 1*, 18. doi: 10.1038/srep00018

Raha, S., Paunesku, T., & Woloschak, G. (2011). Peptide-mediated cancer targeting of nanoconjugates. *Wiley Interdisciplinary Reviews: Nanomedicine and Nanobiotechnology, 3*(3), 269-281. doi: 10.1002/wnan.121

Rahman, W. N., Bishara, N., Ackerly, T., He, C. F., Jackson, P., Wong, C., . . . Geso, M. (2009). Enhancement of radiation effects by gold nanoparticles for superficial radiation therapy. *Nanomedicine, 5*(2), 136-142.

Trono, J. D., Mizuno, K., Yusa, N., Matsukawa, T., Yokoyama, K., & Uesaka, M. (2011). Size, concentration and incubation time dependence of gold nanoparticle uptake into pancreas cancer cells and its future application to X-Ray Drug Delivery System. *J Radiat Res, 52*(1), 103-109.

X-5MonteCarloTeam. (2003a). *MCNP - a general Monte Carlo N-Particle transport code, Version 5: Volume I: Overview and Theory*. Los Alamos National Laboratory.

X-5MonteCarloTeam. (2003b). *MCNP - a general Monte Carlo N-Particle transport code, Version 5: Volume II: User's Guide*. Los Alamos National Laboratory.

X-5MonteCarloTeam. (2003). *MCNP - a general Monte Carlo N-Particle transport code, Version 5: Volume III: Developer's Guide*. Los Alamos National Laboratory.

X-Ray Mass Attenuation Coefficients. Retrieved December 5, 2013, from http://physics.nist.gov/PhysRefData/XrayMassCoef/tab2.html

Yusa, N., Jiang, M., Mizuno, K., & Uesaka, M. (2009). Numerical evaluation of the effectiveness of colloidal gold as a contrast agent. *Radiol Phys Technol, 2*(1), 33-39. doi: 10.1007/s12194-008-0041-2